Solar Energy 213 (2021) 136–144

Contents lists available at ScienceDirect

Solar Energy

journal homepage: www.elsevier.com/locate/solener

Encapsulation improvement and stability of ambient roll-to-roll slot-die-coated organic photovoltaic modules

Ching-Yu Lee [a], Cheng-Si Tsao [a,b,*], Hua-Kai Lin [a], Hou-Chin Cha [a], Tsui-Yun Chung [a], Yun-Ming Sung [c], Yu-Ching Huang [d,*]

[a] Institute of Nuclear Energy Research, Longtan, Taoyuan 32546, Taiwan
[b] Department of Materials Science and Engineering, National Taiwan University, Taipei 10617, Taiwan
[c] Institute of Atomic and Molecular Sciences, Academia Sinica, Taipei 10617, Taiwan
[d] Department of Materials Engineering, Ming Chi University of Technology, New Taipei City 24301, Taiwan

ARTICLE INFO

Keywords:
Organic photovoltaic
Roll-to-roll
Slot-die
Module
Encapsulation
Stability

ABSTRACT

The manufacture of ambient roll-to-roll (R2R) slot-die-coated organic photovoltaic (OPV) is the basis toward commercialization of OPV. The low-cost large-area encapsulation technique of stability improvement of flexible OPV module is under-investigated. The related reports on flexible encapsulation up-scaled from cell were limited. The present study develops an effective and easy encapsulation method and architecture design based on the inverted structure of ambient R2R slot-die-coated PET/ITO/ZnO/active layer/hole transport layer (HTL)/Ag. All module areas are greater than 48 cm^2. The P3HT:PCBM and PV2000:$PC_{71}BM$ adopted as active layers have the performance conversion efficiencies of modules of 1–2.2% and 4.2%, respectively. The thermally-deposited MoO_3 and slot-die-coated PEDOT:PSS HTLs are used to compare the effect of HTL on T_{80} lifetime of the large-area flexible R2R module under the accelerated test. The accelerated stability tests regarding to different encapsulation architectures, including damp-heat and light soaking stresses, were conducted. The intrinsic and extrinsic degradation effects are analyzed. We develop the simple encapsulation design effectively suppressing the lateral ingress of oxygen and moisture. The T_{80} lifetime of P3HT:PCBM-based module can be improved to be 1500 h under the damp-heat test (65 °C/65% RH). The T_{80} lifetime of PV2000:$PC_{71}BM$-based module can last for 7000 h under the dark and ambient environment (30 °C/50 ± 20% RH).

1. Introduction

The solution-processed polymer and organic photovoltaics (OPV) as potential next-generation PV have attracted much attention. The recent development in power conversion efficiency (PCE) of the laboratory-scale single-junction OPV cell demonstrates a rapid progress, exceeding 15% (Cui et al., 2019). One of advantages of OPV technology is the large-area module manufacture with fast speed, high-throughput, low-cost and simple coating or printing methods. Furthermore, the mass production lines using ambient roll-to-roll (R2R) coating on flexible PET substrate and low-cost materials enables significant cost reduction for OPV module compared to the other PV technologies (Angmo et al., 2014), being a critical factor toward commercialization of OPV. The flexible and light-weight R2R-coated OPV modules can offer a variety of diverse applications and commercial opportunities from portable smart electronics and IOT sensors to building-integrated PV. However, there is still a gap from the laboratory scale to the industrial manufacture. The scaling up of OPV module manufacture cause the severe challenges on the control of coating parameters and film/layer interface structure, leading the substantial reduction in performance and bottleneck toward commercialization. Few laboratories or manufacturers devoted to commercial OPV module manufacture. According to the literature (Berny et al., 2016; Lucera et al., 2016), the current PCE of flexible solution-coated polymer solar cell modules with a size of ~100 cm^2 is close to ~5%.

Another bottleneck of OPV commercialization is the stability. The cost, stability and PCE of OPV are usually trade-off. The stability and PCE of large-area OPV module cannot be improved in parallel due to the complex combination and mutual interference of several factors such as the used materials, processing and architecture etc. The PCE of the

* Corresponding authors at: Institute of Nuclear Energy Research, Longtan, Taoyuan, 32546, Taiwan (C.-S. Tsao). Ming Chi University of Technology, New Taipei City 24301, Taiwan (Y.-C. Huang).
E-mail addresses: cstsao@iner.gov.tw (C.-S. Tsao), huangyc@mail.mcut.edu.tw (Y.-C. Huang).

https://doi.org/10.1016/j.solener.2020.11.021
Received 15 June 2020; Received in revised form 19 October 2020; Accepted 7 November 2020
Available online 1 December 2020

P3HT:PCBM module as well-investigated and most-stable OPV system for various degradation tests is 1–2% (Corazza et al., 2015; dos Reis Benattoet al., 2017; Gevorgyan et al., 2011; Roth et al., 2015). Severe instability of the up-scaled OPV module becomes a critical challenge. The understood degradation mechanisms of OPV from the chemical stresses (Cheng and Zhan, 2016; Gevorgyan et al., 2016; Mateker and McGehee, 2017) are categorized as follows: (I) extrinsic degradation caused by chemical reaction with water and oxygen from the atmosphere or ambient environment, (II) intrinsic degradation caused by the temperature or heating in the dark condition, and (III) intrinsic photo-induced degradation. (I) can be reduced by the encapsulation of device. (II) and (III) occur even with perfect encapsulation. The little humidity and oxygen invading through barrier film can significantly accelerate the photo-degradation. The degradation from physical stresses is caused by the tension, shear stress and interfacial stress etc. from the mechanical handling. In general, the strategies improving the overall OPV stability focused on three distinct parts: (1) the core part comprising the donor, acceptor, electrodes and component materials, processing and bulk-heterojunction morphology control of cell device, (2) the device architecture and (3) encapsulation. The most critical defense that offers the OPV stability to an application-ready level is the encapsulation. However, very few reports about the OPV encapsulation are present compared to the large number of efforts on the cell materials and architecture (Angmo et al., 2014). The small-area glass-based OPV cell encapsulated by glass or atomic-layer-deposition (ALD) barrier film demonstrated the excellent stability under the accelerated tests of damp-heat and light soaking (Sapkota et al., 2014). However, the encapsulation of flexible large-area PET-based OPV module suffers the much more difficulties compared to the glass-based OPV. The related researches and reports, which is currently necessary, are relatively very limited.

The flexible encapsulation technique and requirement of OPV module needs to be simple for adapting to the printing industries compared to the complicated and delicate ALD technique. Development of the low-cost, short processing time, simple (easy) encapsulation technique of high OPV stability is proceeding. The usual encapsulation structure for flexible OPB module consists of (1) the polymer-based barrier film and (2) the adhesive bonding the barrier films on the both front and back sides of OPV modules. The low-cost polymer barrier film of 10^{-2}–10^{-3} g m^{-2} day^{-1} of water vapor transmission rate (WVTR) is adopted to effectively enable the OPV modules long-term stability regarding to various degradation stresses (Angmo et al., 2014). Currently, the critical role of encapsulation significantly reducing the stability is the adhesive materials usually having the high WVTR. The different adhesive materials have their own lamination procedure or coating methods, showing the respective characteristics and performance. The commonly used adhesives are pressure sensitive adhesive (PSA) and UV-curable adhesive. The PSA method has been used for a long time to encapsulate flexible R2R-processed OPV modules (Krebs et al., 2011; Krebs et al., 2010). It is shown that the lateral ingress of moisture and oxygen into the module through the adhesive at the edge sides (perimeter) of the encapsulated devices. The additional barrier film with wide PSA edge sealing was developed to inhibit the lateral diffusion of oxygen and moisture such as (Gevorgyan et al., 2013; Hösel et al., 2013; Tanenbaum et al., 2012). Recently, the UV adhesive was additionally adopted to be coated on the edge side of barrier film of PSA-encapsulated OPV modules for inhibiting the lateral diffusion of moisture and oxygen (Weerasinghe et al., 2016). Moreover, it was found that degradation of flexible modules progresses by the penetration of oxygen and moisture through the external metal snap faster as the electric contact/terminal (Gevorgyan et al., 2013; Kim et al., 2016). On the other hand, UV-curable adhesive have been shown to be superior for encapsulation of flexible R2R-coated OPV modules (Angmo et al., 2013). During the encapsulation process, UV exposure and liquid characteristic can effectively eliminate of oxygen from the surface of ZnO particles and modules. The oxidation degradation cause by the ingress of oxygen and moisture through the external contact fastener was observed for almost all PSA-based modules after the accelerated tests, shown the advantage of UV-curing encapsulation over PSA. However, the PSA-based encapsulation has the significant processing advantages over the UV-curing adhesives and is more adapted to integration into different applications (Angmo et al., 2013).

Low-cost PSA and UV-curable adhesives and associated encapsulation methods are necessary toward the commercial OPV mass production. In the review of the advantages and inherent characteristics of PSA and UV-curable adhesive, the present study develops an effective and simple encapsulation method with easy architecture design for flexible OPV modules. The large-area R2R-slot-die-coated OPV modules prepared under the ambient environment are adopted here for evaluating the stability based on this encapsulation architecture. The accelerated stability tests, including damp-heat and light soaking stresses, were conducted for over 1000 h. In this work, the initial PCE values of ambient R2R-coated modules with the different size (48–90 cm^2) based on different donor polymers range from 1% to 4.2%. The encapsulated modules based on different hole-transport layers (HTLs) are also accessed to understand the influence of encapsulation on the modules. The intrinsic and extrinsic degradation effects on the variously prepared modules are analyzed here. We develop the simple encapsulation design without additional barrier film effectively suppressing the lateral ingress of oxygen and moisture through both the lateral sides and narrow channel around the electric contact of the laminated modules. The T_{80} lifetime of flexible P3HT:PCBM-based module can be improved to be 1500 h under an accelerated test at 65 °C/65% RH. The T_{80} lifetime of PV2000:PC_{71}BM-based module can last for 7000 h under the dark and ambient environment (30 °C/50 ± 20% RH).

2. Materials and methods

2.1. Materials preparation

The flexible ITO-coated PET substrate (surface resistance of 15 Ω/square) was received from Optical Filters Ltd. After P1 laser patterning, the ITO/PET substrate was ultrasonically cleaned in acetone and then treated with O_2 plasma for 3 min. For the preparation of ZnO ETL solution, 2.2 g zinc acetate dehydrate (Alfa) and 0.58 g lithium hydroxide monohydrate (Alfa) was dissolved in 100 ml ethanol (Fisher) followed by ultrasonic dispersion for 30 min. Then, 2 ml deionized water was added into the transparent solution followed by stirring at 60 °C for 30 min. The ZnO nanoparticles were dispersed in isopropanol and ethanolamine solution. For the preparation of active layer solution, 15 mg poly(3-hexylthiophene) (P3HT; Rieke Metals) and 15 mg [6,6]-phenyl-C61-butyric acid methyl ester, PC_{61}BM (Sigma-Aldrich) were dissolved in 1 ml O-Xylene (Alfa Aesar) and then stirred at 50 °C for one day under nitrogen-filled glovebox. PEDOT:PSS (CPP 105D) and 1,8-Diiodooctane (DIO) solutions were purchased from Clevios and Aldrich, respectively. The P3HT:PCBM solution has the 1.5% DIO as additive. For preparing the other active layer, 10 mg donor polymer PV2000 (Raynergy Tek. Co. Ltd) and 15 mg PC_{71}BM (Nano-C) were dissolved in 1 ml of solution (Raynergy Tek.) and stirred at 120 °C for one day.

2.2. Roll-to-roll slot-die coating and module fabrication

The P3HT:PC_{61}BM active layer and ZnO ETL were slot-die-coated on the ITO-coated PET substrate under ambient condition (50 ± 20% RH) using Coatema R2R system (Cha et al., 2014; Huang et al., 2016, 2017) with the width of coater of 10.0 cm. The fabricated OPV modules have the inverted structure of PET/ITO/ZnO/P3HT:PC_{61}BM/MoO_3 or PEDOT:PSS/Ag. The ZnO ETL was coated at a speed of 0.5 m/min followed by drying of film through the oven at 150 °C equipped between rollers. The thickness of ETL film is about 30 nm. Then, the active layer with a thickness of ~200 nm is deposited with the coating speed of 1.0 m/min and immediately drying through the oven at between rollers.

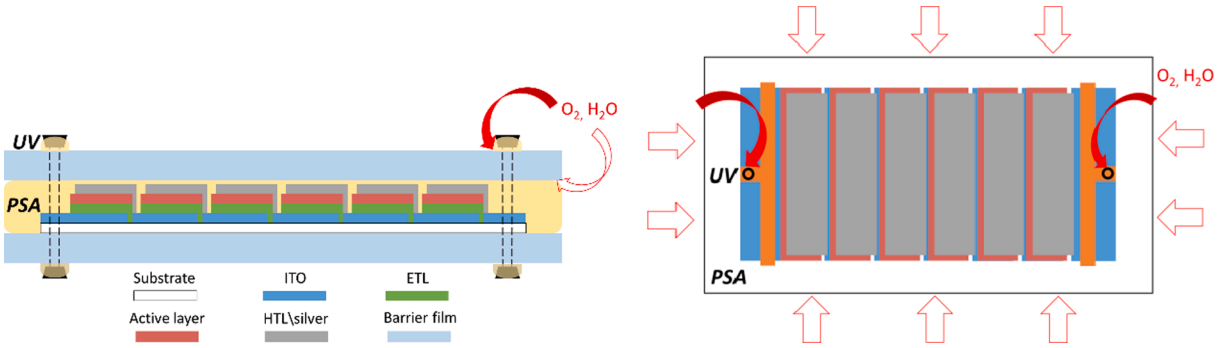

Fig. 1. Crosse section and top view of the module comprised of 6 serially-connected cells. The PSA encapsulation layout and UV-adhesive-protected fastener reduce the lateral penetration of oxygen and moisture.

PEDOT:PSS solution as hole transport layer (HTL) were slot-die-coated on some selected batches. After finishing the coating of each layer, the ITO-PET substrate was rewound for coating the next layer because of the limitation of laboratory-scale coating system. Four modules were cut in a batch. Finally, P2 process was performed by mechanical ablation. The MoO_3 as HTL (~3 nm) and Ag electrode (100 nm) were thermally deposited. P3 ablation lines were carried out by the mask. Some OPV modules were prepared with the P3HT:PC_{61}BM solution with DIO additive for the comparison. The active area of each cell is 1 cm × 8 cm which is defined by the overlap between Ag electrode and ITO. Each module with the active area of 48 cm^2 is comprised of six cells in serial connection. The schematic diagram of module is shown in Fig. 1.

On the other hand, we fabricated the OPV module with the inverted structure of PET/ITO/ZnO/PV2000:PC_{71}BM/MoO_3/Ag. The PV2000:PC_{71}BM active layer is slot-die coated with the speed of 1.2 m/min. The other layers were prepared with the same procedures as the P3HT:PC_{61}BM module under the ambient environment. The PV2000:PC_{71}BM module with active area of 90 cm^2 is comprised of 10 cells in serial connection.

2.3. Encapsulation

Ag tape was applied to terminals connecting the anode and cathode before the encapsulation. 3M™ FTB3-50 film of VWTR < 10^{-3} gm^{-2} day^{-1} was used as the plastic barrier film. The barrier films were bonded onto the front and back sides of the module using PSA (3M™, 467 MP). The PSA was pre-laminated on the full barrier film. All encapsulation materials were pre-conditioned under vacuum at 100 °C for 8 h for removing the residual moisture and oxygen (Weerasinghe et al., 2016; Weerasinghe et al., 2015). The encapsulation process was performed by lamination at 100 °C and a speed of 36 cm/min using office-type laminator (SAMPO). The encapsulated four side (perimeter) around the modules have a width of 1.5 cm to reduce the lateral ingress of oxygen and moisture. Finally, the metal snap fasteners were applied onto Ag tape to provide an electrical contact to the module over the barrier film. The very few amounts of UV adhesive (Egloo, Saes Co.) were smeared around the contact gap between fastener and barrier film for sealing. The encapsulation architecture is shown in Fig. 1. Some modules as the reference were not sealed by UV-adhesive.

2.4. Accelerated tests and performance measurement

Voltage–current curves of the modules prepared here were measured under A.M.1.5 illumination (100 mW/cm^2) using a solar simulator (Abet technologies, Model No 11000). A profiler (AlphaStep D-100, KLA Tencor) was used to measure the real layer thickness. The heating test of the un-capsulated modules was conducted in a nitrogen-filled glove box. The damp-heat test of the encapsulated modules was conducted at 65 °C and 65% RH in an environmental chamber with automatic monitor and constant temperature/humidity control (YEOW LONG Technology developing Co.). This test condition is accordance with SEMI PV76 test standard (SEMI, 2016) (corresponding to ISOS-D-2 (Reese et al., 2011)). Light-soaking test in ambient condition is conducted under the continuous AM 1.5G solar illumination (100 mW cm^{-2}) monitored by a photodetector (Model: KD-LS01-0808, King Design Industrial Co. Ltd). The illumination area is 40 cm × 40 cm with cut of an UV filter (400 nm).

3. Result and discussions

Fig. 2 shows the images of the flexibly encapsulated P3HT:PCBM-based modules with the active area of 48 cm^2. The PCE values of all R2R-slot-die-coated P3HT:PCBM modules fabricated under ambient condition are 1–2% based on MoO_3 HTL and ~2.5% based on PEDOT:PSS HTL, respectively. The TEM cross section image of the module is shown in Fig. 3. First of all, the un-encapsulated and encapsulated modules stored at 65 °C for 1800 h under a dark and nitrogen-filled environment (as reference group) demonstrate the stable photovoltaic

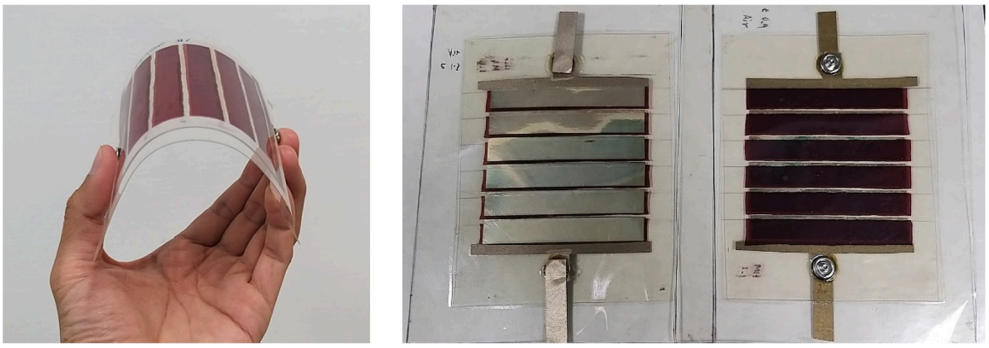

Fig. 2. Photographic images of the flexible encapsulated modules.

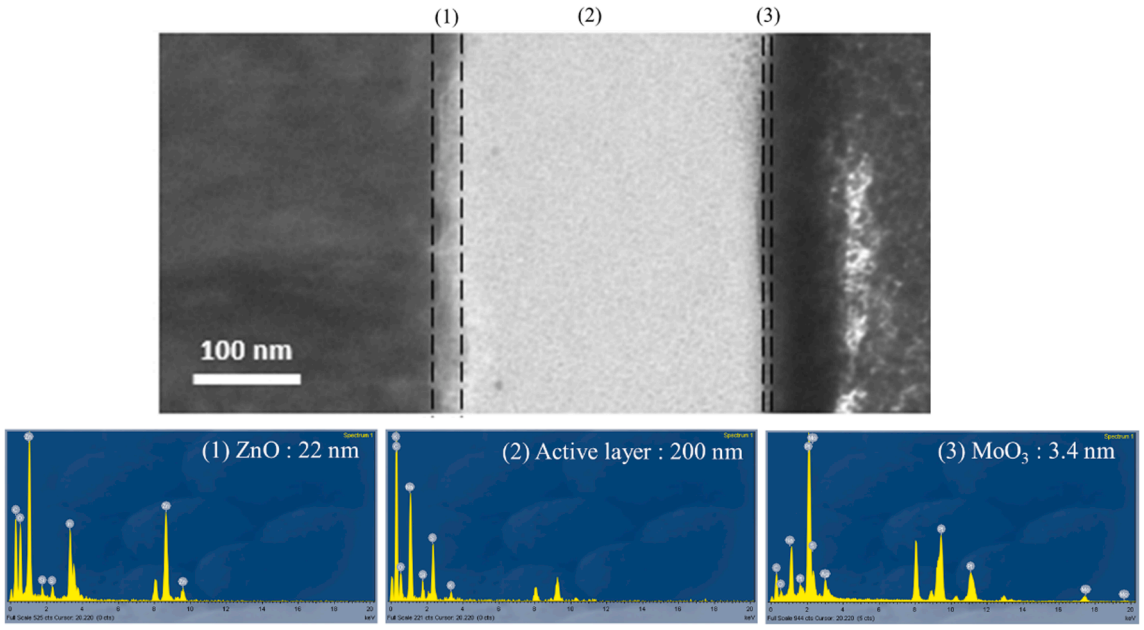

Fig. 3. TEM cross section image of the module with labelled thickness for each layer and their corresponding EDX spectrum of layers.

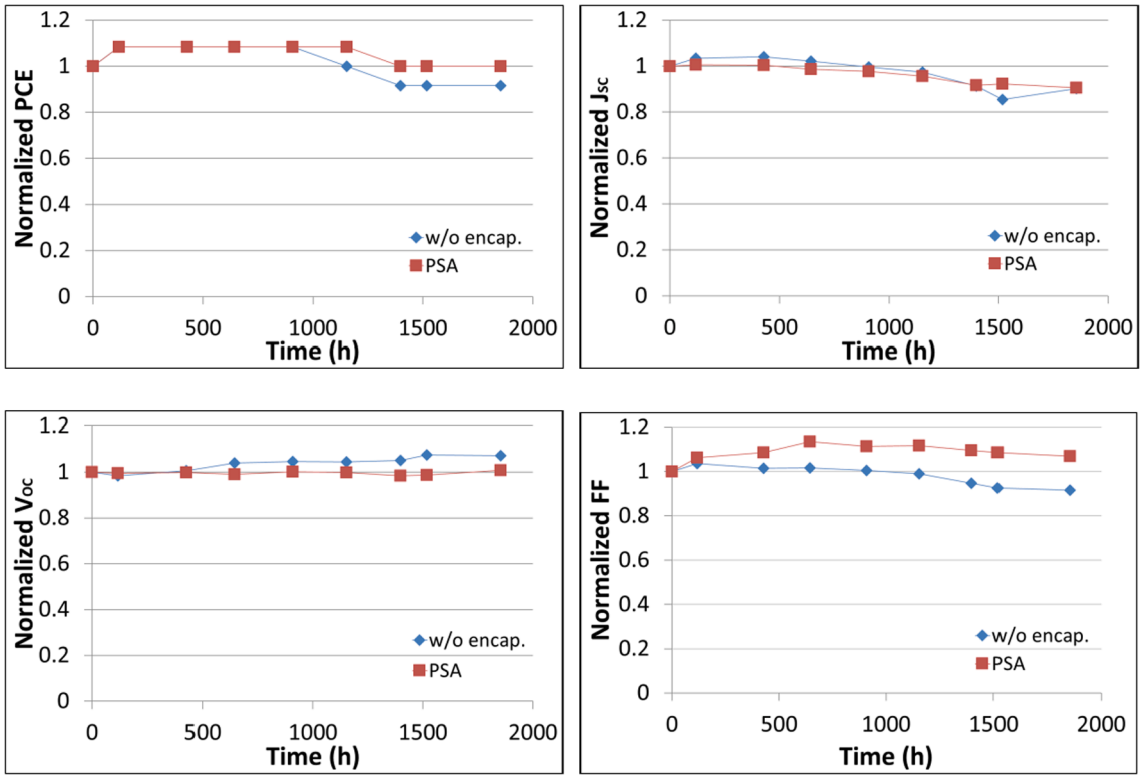

Fig. 4. Variation of photovoltaic parameters with aging time for the un-encapsulated and encapsulated modules based on the structure of P3HT:PCBM/MoO_3/Ag under an accelerated test at 65 °C.

characteristics with a T_{80} lifetime (The time reaching 80% of initial PCE) more than 1800 h, as shown in Fig. 4. The stability curve of un-encapsulated module demonstrates that the R2R slot-die-coated module has good resistance against the intrinsic degradation at 65 °C. The encapsulated module keeps same PCE degradation and shows there are (1) no residual oxygen and moisture within the encapsulation materials damaging the module during the test (Weerasinghe et al., 2016, 2015), and (2) the additional damage from the lamination of barrier film. It seems that the hot pressure of encapsulation may slightly improve the contact of layer interface and facilitate long-term stability according to the comparison of two curves. This typical stable performance under the nitrogen-environment and dark storage at 65 °C can be observed over the several batches of modules. The PCEs of two modules are ~1.2%. Corresponding current–voltage measurements of the flexible modules before and after this thermal-aging degradation test is shown in Fig. 5.

For the accelerated test under 65 °C/65% RH (SEMI PV76 or ISOS-

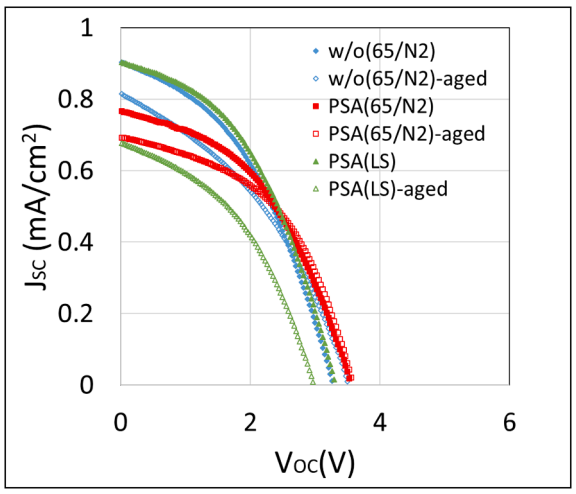

Fig. 5. Current-voltage measurements of the flexible modules before and after the thermal-aging and light-soaking degradation tests corresponding to Figs. 4 and 13.

D2) condition, three encapsulation designs for investigation stability are (1) the un-encapsulated module, (2) the module only with barrier film encapsulation using PSA (named PSA-based), (3) the module with barrier film encapsulation using PSA and additional UV-curable adhesive around snap fastener (named PSA + UV-based), as shown in Fig. 1. The corresponding stability curves over aging time for each encapsulation design are based on two or more modules. The variation of photovoltaic parameters with aging time of representative modules is shown in Fig. 6. Corresponding current–voltage measurements of the flexible modules before and after the accelerated test is shown in Fig. 7. Laser beam induced current (LBIC) characterization result of the seriously degraded PSA-encapsulated P3HT:PCBM module after the accelerated test at 65 °C/65% RH test is shown in Fig. 8. The failure of some modules on the accelerated test (not shown here) is due to the defects resulted from the manual handling of encapsulation. The initial PCEs of the un-encapsulated, PSA-based encapsulated and PSA + UV-based encapsulated modules are 1.4%. The PSA-based module has the open-circuit voltage (V_{oc}), short-circuit current (J_{sc}) and fill factor (FF) of 3.70 V, 0.88 mA/cm^2 and 44.1%, respectively. The PSA + UV-based module has the V_{oc}, J_{sc} and FF of 3.61 V, 0.86 mA/cm^2 and 44.5%, respectively. The normalized PCE and FF of the un-encapsulated module under 65 °C/65% RH condition dramatically drop to ~70% of initial values within few hours (i.e., burn-in degradation) followed by the gradual decrease to 40% of initial PCE after 1000 h and then a stable behavior up to 1800 h. In contrast, the J_{sc} demonstrates a significantly linear decay, being a

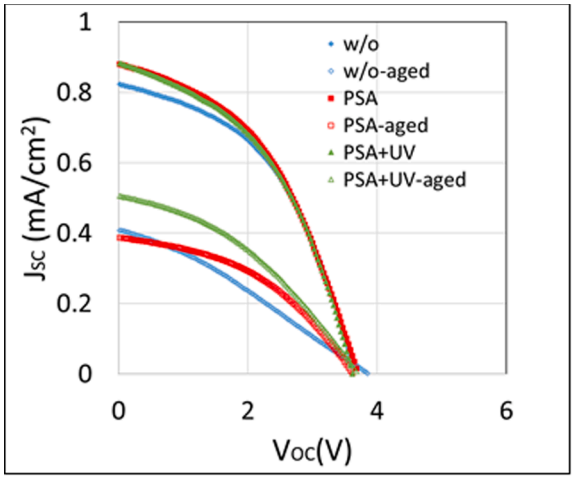

Fig. 7. Current-voltage measurements of the modules before and after the accelerated test at 65 °C/65% RH test corresponding to Fig. 6.

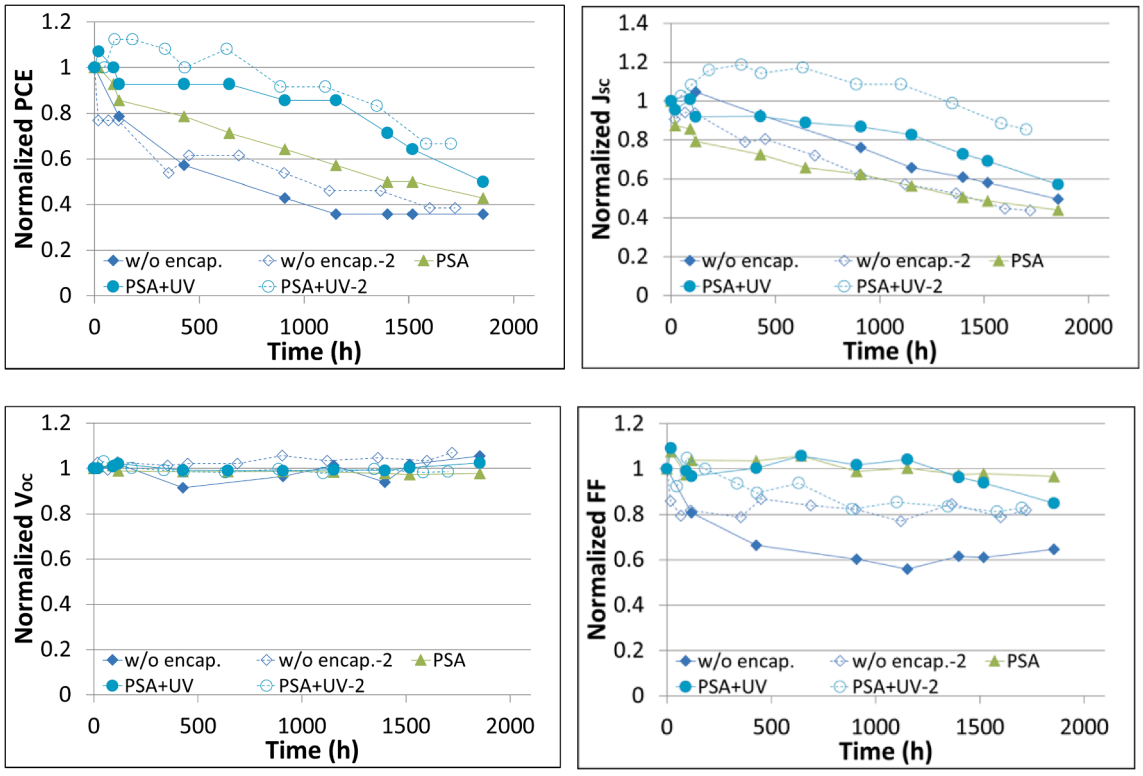

Fig. 6. Variation of photovoltaic parameters with aging time for the modules with different encapsulation architectures under an accelerated test at 65 °C °C/65% RH. The additional modules named by w/o encap-2 and PSA + UV-2 are from the same test batch, showing the variation due to fabrication process.

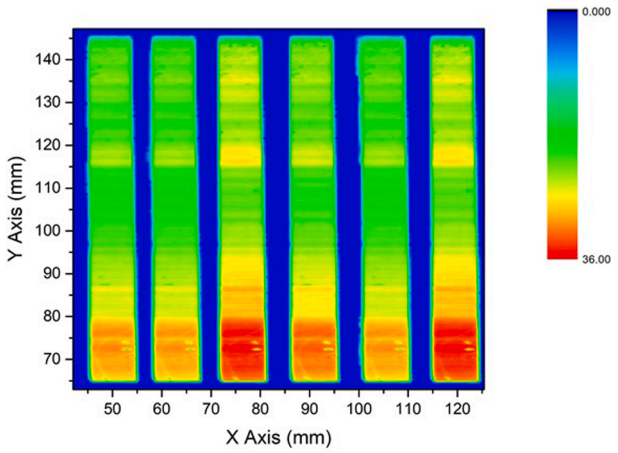

Fig. 8. LBIC characterization of the seriously degraded PSA-encapsulated P3HT:PCBM module after the accelerated test at 65 °C/65% RH test. The green region shows the serve degradation by the ingress of moisture. (For interpretation of the references to colour in this figure legend, the reader is referred to the web version of this article.)

major factor of decay in the PCE during the long-term stability test. Notably, the V_{oc} almost does not vary during the test period. The un-encapsulated (or control) module provides the most serious degradation data suffering the ingress of oxygen and humidity. The initial drop and linear decay of FF and Jsc, respectively, can be contributed sequentially to the (1) degradation (oxidation and expansion) of porous interface between the solution-processed ZnO ETL and active layer due to the fast diffusion of oxygen and moisture via the channel between layer interfaces, (2) oxidation degradation of ZnO ETL and Ag electrode in depth direction. In the present study, the stable behavior of V_{oc} during aging time can be explained by little degradation of the active layer. Two reasons are (1) the previously accelerated test under 65 °C/nitrogen condition demonstrated the good stability against the intrinsic degradation, and (2) the thermal evaporated MoO3 was used as HTL instead of the well-used PEDOT:PSS HTL. The current R2R-coated modules usually adopted the inverted structure with PEDOT:PSS (HTL)/Ag electrode on the active layer. These PEDOT:PSS HTL-based modules under accelerated test demonstrated the V_{oc} gradually decline with the aging time (Angmo et al., 2013; Gevorgyan et al., 2013; Kim et al., 2016; Tanenbaum et al., 2012; Weerasinghe et al., 2016). Several studies about these modules pointed out that the absorption of moisture by hygroscopic PEDOT:PSS as major factor of degradation causes the oxidation (Gevorgyan et al., 2013; Tanenbaum et al., 2012) at interfaces and expansion (Cui et al., 2019) of the PEDOT:PSS followed by the PSS polymer as an acid (SO_3H molecules) diffusing into the active layer and ZnO ETL and leading to chemical and morphological changes (Kim et al., 2016). The other degradation factors include the oxidation of metal electrode or contact near the terminal of module (Angmo et al., 2013; Kim et al., 2016; Mateker and McGehee, 2017). The real mechanism of degradation in OPV module is complex due to the several competing mechanisms from various layers and interfaces. The review article reported that the OPV device MoO_3 HTL with has the much longer T_{80} lifetime by an order than that with PEDOT:PSS HTL under accelerated test (Reese et al., 2011). The difference between T_{80} lifetimes of both kinds of devices largely increased with increasing the humidity up to two orders at the humidity of greater than 60% RH.

The PSA-based module under 65 °C/65% RH condition demonstrated an initial burn-in degradation within few days and then the linear decline to 60% of its initial PCE after 1000 h. The T_{80} lifetime is 500 h. In contrast, the PCE of PSA + UV-based module demonstrated a stable behavior within 1200 h after the initial burn-in degradation, indicating the T_{80} lifetime of ~1200 h. The main cause of degradation of PSA-based module can be attributed to the ingress of oxygen and

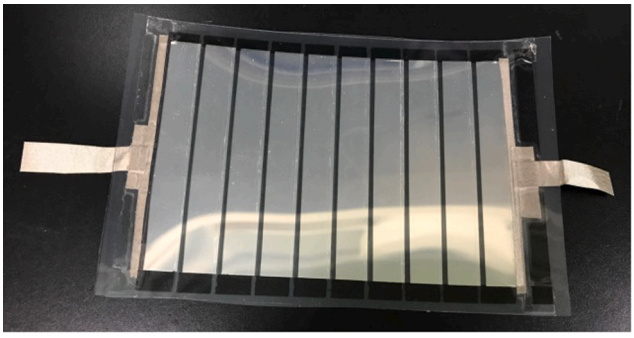

Fig. 9. Photographic image of the flexible inverted PV2000:$PC_{71}BM$ modules (10 cells in serial connection, each cell has the area of 1 cm × 9 cm).

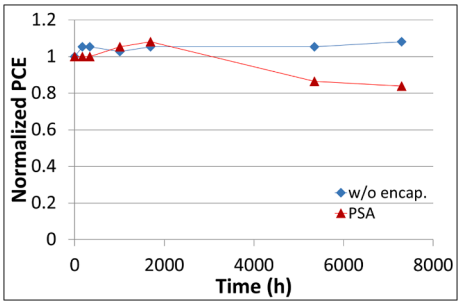

Fig. 10. Stability curve of the un-encapsulated (nitrogen environment) and encapsulated modules (50 ± 20% RH ambient environment) over the storage time.

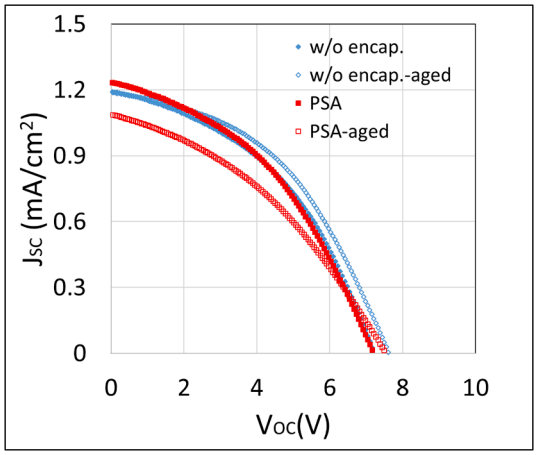

Fig. 11. Current-voltage measurements of the PV2000:$PC_{71}BM$ modules before and after the degradation test corresponding to Fig. 10.

moisture through the channel around metal fastener. It is demonstrated that few UV adhesive covering the channel can effectively reduce the ingress of oxygen and moisture. The degradation of PSA + UV-based module is also related to the ingress via UV-adhesive-covered channel as well as the PSA-sealed side. Similar to the variation of V_{oc}, the stable behavior of FF with increasing the aging time can be explained by use of the MoO_3 HTL rather than the PEDOT:PSS HTL.

On the other hand, the flexible PV2000:$PC_{71}BM$ module with an active area of 90 cm^2 is adopted as a reference comparing the influence of metal snap fastener. The module was encapsulated by PSA with side width of 1.5 cm. The Ag tape as the electrode terminal was extended to the outside of module instead of the use of metal snap fastener, as shown in Fig. 9. The extension of Ag tape causes the increase of electrode

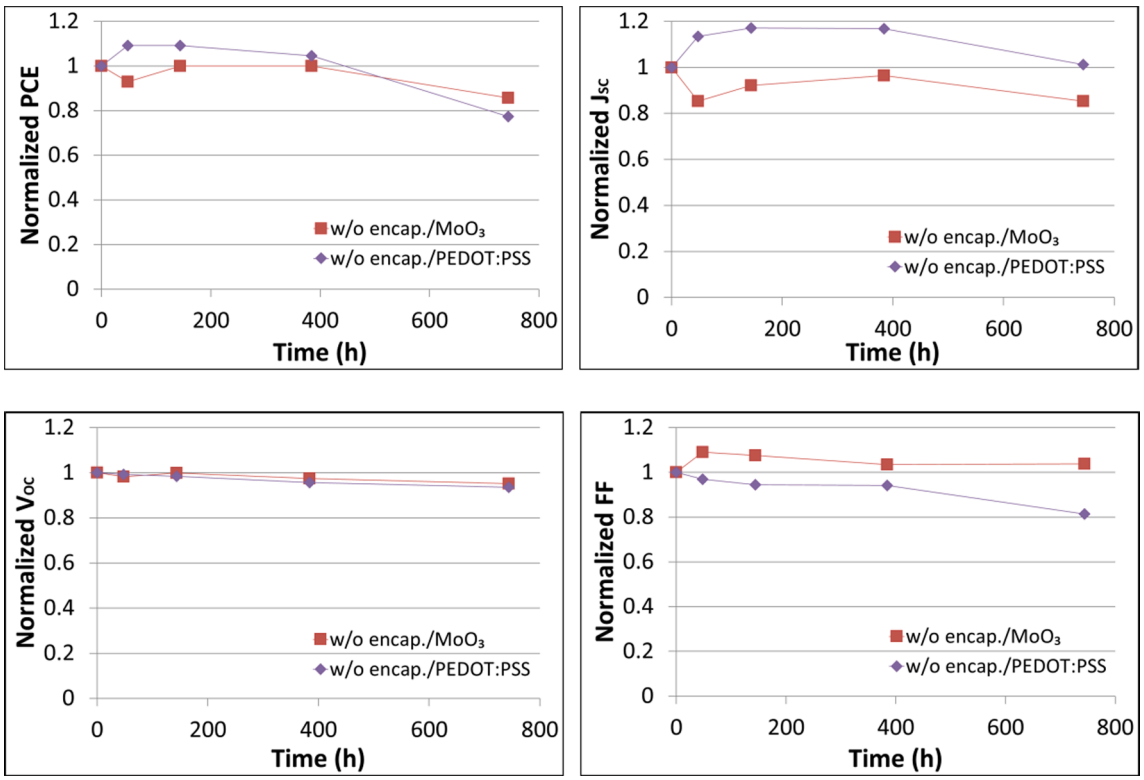

Fig. 12. Variation of photovoltaic parameters with aging time for the MoO_3- and PEDOT:PSS-based modules under a dark and nitrogen environment at 85 °C.

contact impedance and reduces the PCE. The PCE of the un-encapsulated module is 4.2%. This module was stored under a dark and nitrogen condition at 25 °C for serving a reference module. The PCE of the encapsulated module is 3.8% which was stored under a dark and ambient environment at 25–32 °C/50 ± 20% RH. The variation of photovoltaic parameters of both modules with storage time is shown in

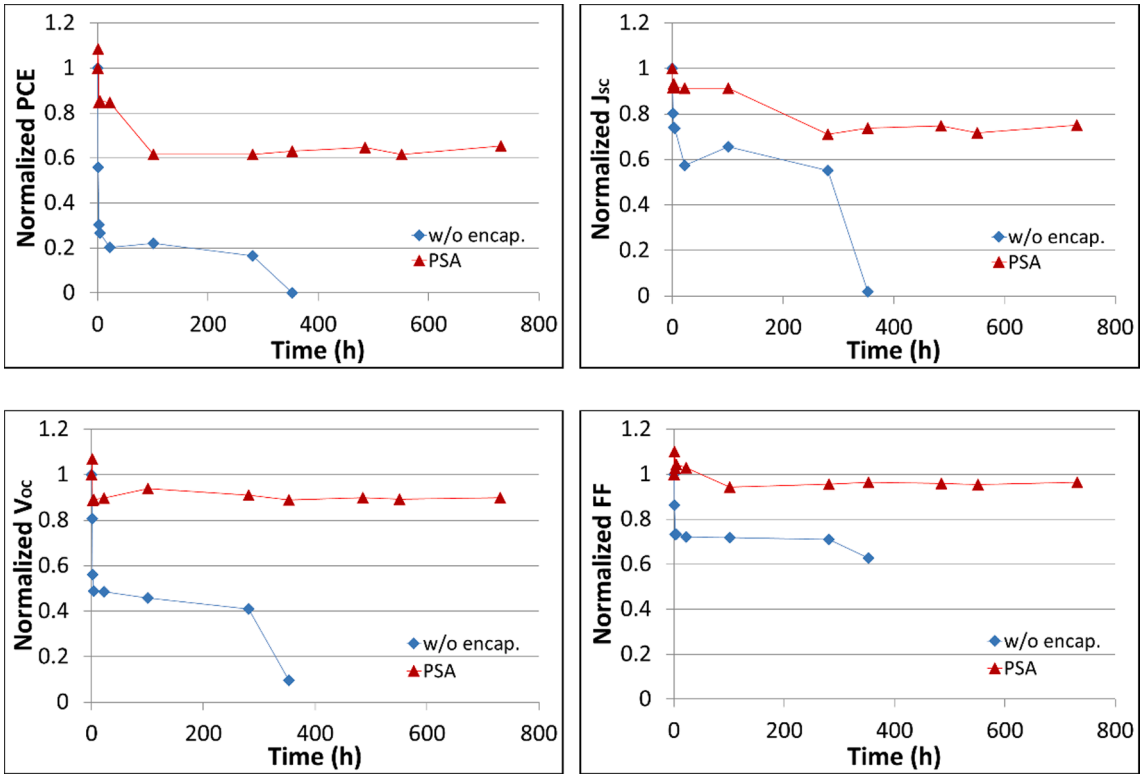

Fig. 13. Variation of photovoltaic parameters with light-soaking time for the un-encapsulated and PSA-sealed modules with MoO_3 HTL under the continuous illumination of AM1.5G.

Fig. 10. Corresponding current–voltage measurements of the flexible modules before and after the storage is shown in Fig. 11. The encapsulated module under the ambient environment with high humidity exhibits 7000 h of T_{80} lifetime. The other module under the nitrogen environment has a stable behavior and remains the initial PCE during this period (7000 h). This result suggests that the diffusion of oxygen and moisture into module through the four PSA-encapsulated sides of module plays an important role in degradation (i.e., extrinsic degradation). The ingress through the channel around the metal fastener is a main factor of degradation by the comparison between the architecture designs of previous P3HT:PCBM modules and PV2000 module.

Two inverted P3HT:PCBM modules (48 cm^2 for each module) with the thermally deposited MoO_3 HTL and slot-die-coated PEDOT:PSS HTL, respectively, were stored under a dark and nitrogen environment at 85 °C for the accelerated test of intrinsic degradation. Because the slot-die-coated PEDOT:PSS HTL has a higher conductivity for combining the grid Ag electrode in the future, the PCE of the PEDOT:PSS-based module is 2.2% higher than that of MoO_3-based module (1.4%). The variation of photovoltaic parameters of these modules with aging time is shown in Fig. 12. Both modules exhibit the similar T_{80} lifetime of ~800 h, showing that factors of thermal degradation are (1) from the active layer due to the thermally-unstable BHJ structure and (2) diffusion of Ag atoms of electrode into the active layer and HTL. This result suggests that the thermal degradation mechanism of both modules is the same. The T_{80} lifetime is mainly subjected to the processing of active layer. However, the T_{80} lifetime of modules is substantially reduced to 200 h under the ambient environment at 85 °C/~40% RH.

The photo-oxidation stability of module is also subject to the ingress of oxygen and moisture from the ambient environment, being affected by the quality of encapsulation. Fig. 13 shows the degradation curve of the un-encapsulated and PSA-sealed modules with MoO_3 HTL as a function of light-soaking time under the ambient environment and continuous illumination of AM1.5G. The initial PCEs of both modules are 1.1% and 1.3%. For the un-encapsulated module, the burn-in degradation due to the light soaking occurred within a very short time and the PCE dramatically drop to 20% of initial value. For the PSA-sealed module, the burn-in degradation due to the light soaking occurred within 100 h and the PCE dramatically drop to 60% of initial value. The result shows that the photo-oxidation could substantially degrade the un-encapsulated module due to the full exposure to oxygen and moisture. The burn-in degradation of the encapsulated P3HT:PCBM module might be due to the addition of additive DIO.

4. Conclusion

The large-area R2R-slot-die-coated inverted module with MoO_3 HTL could keep Voc value as well as FF stable during the PCE decayed under the under the damp-heat test (65 °C/65% RH). The extrinsic degradation due to the ingress of oxygen and moisture is the main factor compared to the intrinsic degradation caused by high temperature. The lateral ingress of oxygen and moisture through narrow channel around the electric contact of the laminated modules is more critical than that through the laminated module sides. The simple encapsulation design with least barrier films developed here can effectively suppress the ingress. The present study provides the strategy of flexible encapsulation or strengthening design focused on the suppression to all possible diffusional paths in the lateral sides of modules without additional barrier. The resistance against the ingress of oxygen and moisture largely decreased at 85 °C which is also a current challenge for the other encapsulation studies. It seems that the exploration of good capability of adhesive at high temperature is highly desirable.

Declaration of Competing Interest

The authors declare that they have no known competing financial interests or personal relationships that could have appeared to influence the work reported in this paper.

Acknowledgements

This work was financial supported by Ministry of Science and Technology of Taiwan (MOST 107-2218-E-131-007-MY3, MOST 109-2622-E-131-004 -CC3) and Academia Sinica (AS-SS-109-05).

References

Angmo, D., Gevorgyan, S.A., Larsen-Olsen, T.T., Søndergaard, R.R., Hösel, M., Jørgensen, M., Gupta, R., Kulkarni, G.U., Krebs, F.C., 2013. Scalability and stability of very thin, roll-to-roll processed, large area, indium-tin-oxide free polymer solar cell modules. Org. Electron. 14 (3), 984–994.

Angmo, D., Sommeling, P., Gupta, R., Hösel, M., Gevorgyan, S., Kroon, J., Kulkarni, G., Krebs, F., 2014. Outdoor operational stability of indium-free flexible polymer solar modules over 1 year studied in India, Holland, and Denmark. Adv. Eng. Mater. 16, 976–987.

Berny, S., Blouin, N., Distler, A., Egelhaaf, H.-J., Krompiec, M., Lohr, A., Lozman, O.R., Morse, G.E., Nanson, L., Pron, A., Sauermann, T., Seidler, N., Tierney, S., Tiwana, P., Wagner, M., Wilson, H., 2016. Solar trees: First large-scale demonstration of fully solution coated, semitransparent, flexible organic photovoltaic modules. Adv. Sci. 3 (5), 1500342.

Cha, H.-C., Huang, Y.-C., Hsu, F.-H., Chuang, C.-M., Lu, D.-H., Chou, C.-W., Chen, C.-Y., Tsao, C.-S., 2014. Performance improvement of large-area roll-to-roll slot-die-coated inverted polymer solar cell by tailoring electron transport layer. Sol. Energy Mater. Sol. Cells 130, 191–198.

Cheng, P., Zhan, X., 2016. Stability of organic solar cells: challenges and strategies. Chem. Soc. Rev. 45 (9), 2544–2582.

Corazza, M., Krebs, F.C., Gevorgyan, S.A., 2015. Lifetime of organic photovoltaics: Linking outdoor and indoor tests. Sol. Energy Mater. Sol. Cells 143, 467–472.

Cui, Y., Yao, H., Zhang, J., Zhang, T., Wang, Y., Hong, L., Xian, K., Xu, B., Zhang, S., Peng, J., Wei, Z., Gao, F., Hou, J., 2019. Over 16% efficiency organic photovoltaic cells enabled by a chlorinated acceptor with increased open-circuit voltages. Nat. Commun. 10 (1), 2515.

dos Reis Benatto, G.A., Corazza, M., Roth, B., Schütte, F., Rengenstein, M., Gevorgyan, S. A., Krebs, F.C., 2017. Inside or outside? Linking outdoor and indoor lifetime tests of ITO-free organic photovoltaic devices for greenhouse applications. Energy Technol. 5 (2), 338–344.

Gevorgyan, S.A., Madsen, M.V., Dam, H.F., Jørgensen, M., Fell, C.J., Anderson, K.F., Duck, B.C., Mescheloff, A., Katz, E.A., Elschner, A., Roesch, R., Hoppe, H., Hermenau, M., Riede, M., Krebs, F.C., 2013. Interlaboratory outdoor stability studies of flexible roll-to-roll coated organic photovoltaic modules: Stability over 10,000h. Sol. Energy Mater. Sol. Cells 116, 187–196.

Gevorgyan, S.A., Madsen, M.V., Roth, B., Corazza, M., Hösel, M., Søndergaard, R.R., Jørgensen, M., Krebs, F.C., 2016. Lifetime of organic photovoltaics: Status and predictions. Adv. Energy Mater. 6 (2), 1501208.

Gevorgyan, S.A., Medford, A.J., Bundgaard, E., Sapkota, S.B., Schleiermacher, H.-F., Zimmermann, B., Würfel, U., Chafiq, A., Lira-Cantu, M., Swonke, T., Wagner, M., Brabec, C.J., Haillant, O., Voroshazi, E., Aernouts, T., Steim, R., Hauch, J.A., Elschner, A., Pannone, M., Xiao, M., Langzettel, A., Laird, D., Lloyd, M.T., Rath, T., Maier, E., Trimmel, G., Hermenau, M., Menke, T., Leo, K., Rösch, R., Seeland, M., Hoppe, H., Nagle, T.J., Burke, K.B., Fell, C.J., Vak, D., Singh, T.B., Watkins, S.E., Galagan, Y., Manor, A., Katz, E.A., Kim, T., Kim, K., Sommeling, P.M., Verhees, W.J. H., Veenstra, S.C., Riede, M., Greyson Christoforo, M., Currier, T., Shrotriya, V., Schwartz, G., Krebs, F.C., 2011. An inter-laboratory stability study of roll-to-roll coated flexible polymer solar modules. Sol. Energy Mater. Sol. Cells 95 (5), 1398–1416.

Hösel, M., Søndergaard, R.R., Jørgensen, M., Krebs, F.C., 2013. Comparison of UV-curing, hotmelt, and pressure sensitive adhesive as roll-to-roll encapsulation methods for polymer solar cells. Adv. Eng. Mater. 15 (11), 1068–1075.

Huang, Y.-C., Cha, H.-C., Chen, C.-Y., Tsao, C.-S., 2016. Morphological control and performance improvement of organic photovoltaic layer of roll-to-roll coated polymer solar cells. Sol. Energy Mater. Sol. Cells 150, 10–18.

Huang, Y.-C., Cha, H.-C., Chen, C.-Y., Tsao, C.-S., 2017. A universal roll-to-roll slot-die coating approach towards high-efficiency organic photovoltaics. Prog. Photovoltaics Res. Appl. 25 (11), 928–935.

Kim, S.H., Son, H.J., Park, S.H., Hahn, J.S., Kim, D.H., 2016. A study for degradation of flexible organic photovoltaic modules via damp-heat test: By accessing individual layers of the module. Sol. Energy Mater. Sol. Cells 144, 187–193.

Krebs, F.C., Fyenbo, J., Tanenbaum, D.M., Gevorgyan, S.A., Andriessen, R., van Remoortere, B., Galagan, Y., Jørgensen, M., 2011. The OE-A OPV demonstrator anno domini 2011. Energy Environ. Sci. 4 (10), 4116–4123.

Krebs, F.C., Tromholt, T., Jørgensen, M., 2010. Upscaling of polymer solar cell fabrication using full roll-to-roll processing. Nanoscale 2 (6), 873–886.

Lucera, L., Machui, F., Kubis, P., Schmidt, H.D., Adams, J., Strohm, S., Ahmad, T., Forberich, K., Egelhaaf, H.J., Brabec, C.J., 2016. Highly efficient, large area, roll coated flexible and rigid OPV modules with geometric fill factors up to 98.5% processed with commercially available materials. Energy Environ. Sci. 9 (1), 89–94.

Mateker, W.R., McGehee, M.D., 2017. Progress in understanding degradation mechanisms and improving stability in organic photovoltaics. Adv. Mater. 29 (10), 1603940.

Reese, M.O., Gevorgyan, S.A., Jørgensen, M., Bundgaard, E., Kurtz, S.R., Ginley, D.S., Olson, D.C., Lloyd, M.T., Morvillo, P., Katz, E.A., Elschner, A., Haillant, O., Currier, T.R., Shrotriya, V., Hermenau, M., Riede, M., Kirov, K.R., Trimmel, G., Rath, T., Inganäs, O., Zhang, F., Andersson, M., Tvingstedt, K., Lira-Cantu, M., Laird, D., McGuiness, C., Gowrisanker, S., Pannone, M., Xiao, M., Hauch, J., Steim, R., DeLongchamp, D.M., Rösch, R., Hoppe, H., Espinosa, N., Urbina, A., Yaman-Uzunoglu, G., Bonekamp, J.-B., van Breemen, A.J.J.M., Girotto, C., Voroshazi, E., Krebs, F.C., 2011. Consensus stability testing protocols for organic photovoltaic materials and devices. Sol. Energy Mater. Sol. Cells 95 (5), 1253–1267.

Roth, B., dos Reis Benatto, G.A., Corazza, M., Søndergaard, R.R., Gevorgyan, S.A., Jørgensen, M., Krebs, F.C., 2015. The critical choice of PEDOT:PSS additives for long term stability of roll-to-roll processed OPVs. Adv. Energy Mater. 5 (9), 1401912.

Sapkota, S.B., Spies, A., Zimmermann, B., Dürr, I., Würfel, U., 2014. Promising long-term stability of encapsulated ITO-free bulk-heterojunction organic solar cells under different aging conditions. Sol. Energy Mater. Sol. Cells 130, 144–150.

SEMI PV76 – Test Method for Durability of Low Light Intensity Organic Photovoltaic (OPV) and Dye-Sensitized Solar Cell (DSSC). Photovoltaic.

Tanenbaum, D.M., Dam, H.F., Rösch, R., Jørgensen, M., Hoppe, H., Krebs, F.C., 2012. Edge sealing for low cost stability enhancement of roll-to-roll processed flexible polymer solar cell modules. Sol. Energy Mater. Sol. Cells 97, 157–163.

Weerasinghe, H.C., Vak, D., Robotham, B., Fell, C.J., Jones, D., Scully, A.D., 2016. New barrier encapsulation and lifetime assessment of printed organic photovoltaic modules. Sol. Energy Mater. Sol. Cells 155, 108–116.

Weerasinghe, H.C., Watkins, S.E., Duffy, N., Jones, D.J., Scully, A.D., 2015. Influence of moisture out-gassing from encapsulant materials on the lifetime of organic solar cells. Sol. Energy Mater. Sol. Cells 132, 485–491.